Brain Research Bulletin 156 (2020) 10–14

Contents lists available at ScienceDirect

Brain Research Bulletin

journal homepage: www.elsevier.com/locate/brainresbull

The fluorescent dye 3,3′-diethylthiatricarbocyanine iodide is unsuitable for *in vivo* imaging of myelination in the mouse

Bálint Botz[a,b], István Zoárd Bátai[a,c], Tamás Kiss[a], Erika Pintér[a,c], Zsuzsanna Helyes[a,c], Kata Bölcskei[a,c,*]

[a] *János Szentágothai Research Centre and Centre for Neuroscience, University of Pécs, H-7624 Pécs, Ifjúság út 20, Hungary*
[b] *Department of Radiology, University of Pécs Medical School, H-7624 Pécs, Ifjúság út 13, Hungary*
[c] *Department of Pharmacology and Pharmacotherapy, University of Pécs Medical School, H-7624 Pécs, Szigeti út 12, Hungary*

ARTICLE INFO

Keywords:
3,3′-diethylthiatricarbocyanine iodide
In vivo optical imaging
Myelination
Blood-brain barrier

ABSTRACT

There is a growing interest to use non-invasive optical imaging methods to study central nervous system diseases. The application of a myelin-binding fluorescent dye, 3,3-diethylthiatricarbocyanine iodide (DBT) was recently described for *in vivo* optical imaging of demyelination in the mouse. In the present study we aimed at adapting the method to our optical imaging systems, the IVIS Lumina II to measure epifluorescence and the fluorescent molecular tomograph (FMT) for 3-dimensional quantification of the fluorophore.

Epifluorescent imaging was performed 5 – 30 min after DBT injection which was followed by FMT imaging at 40 min. Two mice also underwent micro-CT imaging in the FMT cassette for the purpose of FMT-CT co-registration. *Ex vivo* imaging of the brain and other tissues of the head and neck was carried out 1 h after injection.

Both the FMT-CT co-registration and the *ex vivo* imaging of organs proved that DBT poorly crossed the blood-brain barrier. The dye did not accumulate in the myelin sheath of the sciatic nerve. In contrast, there was an intense accumulation in the pituitary and salivary glands. The FMT-CT co-registration unequivocally demonstrated that the signal localized to the head did not originate from beyond the blood-brain barrier. No myelin binding was demonstrated by the *ex vivo* imaging either.

In conclusion, DBT is unsuitable for *in vivo* imaging of myelination due to its poor BBB penetration, accumulation in other structures of the head and neck region and lack of selective binding towards myelin *in vivo*.

1. Introduction

There is a growing interest for versatile molecular imaging methods allowing to assess the development and course of preclinical models of central nervous system (CNS) disorders in a non-invasive manner. Nuclear imaging techniques, such as positron emission tomography (PET), single photon emission tomography (SPECT) and magnetic resonance imaging (MRI), are the gold standards of the field. Meanwhile, optical imaging offers additional benefits by seamlessly allowing *in vivo* and *ex vivo* imaging using the same tracers, comparatively easy development of novel imaging biomarkers, and simultaneous imaging of multiple contrast agents with distinct optical parameters. Furthermore, optical imaging equipment have comparably modest lab footprint and operational costs compared to the above listed methods (Hillman, 2007; Willmann et al., 2008).

Abnormal myelination is a hallmark feature of several CNS diseases such as multiple sclerosis, therefore blood-brain barrier (BBB)-permeable optical imaging tracers demonstrating selectivity towards myelin could become valuable tools for imaging brain disease models in rodents. 3,3-diethylthiatricarbocyanine iodide (DBT/DTTCI/Cy7) is a near infrared (NIR) fluorescent dye that was reported to cross the BBB and bind selectively to myelin, thereby allowing selective *in vivo* imaging of de/remyelination in murine models (Schmitz et al., 2014; Wang et al., 2011).

We have recently aimed at implementing the method in our facility using two optical imaging systems, the IVIS Lumina II to measure epifluorescence and the fluorescent molecular tomograph (FMT 2000) for precise quantification of the fluorophore. Since fluorescence imaging is a tracer-based technique where anatomical information is not inherently present, co-localization using morphological imaging is crucial

Abbreviations: DTTCI / DBT, 3,3′-diethylthiatricarbocyanine iodide; BBB, blood-brain barrier; NIR, near infrared; IVIS, *in vivo* imaging system; FMT, fluorescent molecular tomograph; ROI, region of interest

* Corresponding author at: University of Pécs, Medical School, Department of Pharmacology and Pharmacotherapy, H-7624 Pécs, Szigeti út 12, Hungary.
E-mail address: kata.bolcskei@aok.pte.hu (K. Bölcskei).

https://doi.org/10.1016/j.brainresbull.2019.12.009
Received 14 August 2019; Received in revised form 7 December 2019; Accepted 13 December 2019
Available online 16 December 2019

in case of complex anatomical structures being interrogated. Prior studies about the *in vivo* applications of DBT have used epifluorescence and x-ray imaging which are however both two-dimensional, and therefore cannot reliably establish the three-dimensional position of the signal source. Thus, in the present study we have combined the FMT imaging with micro-computer tomography in order to establish the position of the fluorescent tracer and its relation to anatomical structures in three dimensions. In the present paper, we show results of our validation process which provides clear evidence for the need to re-evaluate this seemingly promising myelin-imaging method.

2. Materials and methods

2.1. Animals

Six-week-old NMRI mice (weighing 35 − 40 g) were used for the experiments. The original breeding pairs were obtained from Charles River (Sulzfeld, Germany). The animals were bred in the Laboratory Animal House of the Department of Pharmacology and Pharmacotherapy at the University of Pécs, fed with standard rodent chow and water *ad libitum*, kept at 24 − 25 °C ambient temperature and 12 h light-dark cycles. The studies were carried out according to the EU Directive 2010/63/EU on the protection of animals used for scientific purposes and approved by the Ethics Committee on Animal Research of the University of Pécs according to the Ethical Codex of Animal Experiments (license No: BA02/2000-17/2016).

2.2. Imaging protocol

DBT (Sigma-Aldrich) was dissolved in DMSO to yield a stock solution of 10 mg/ml, which was further diluted to 0.06 mg/ml with sterile PBS (final DMSO concentration was 0.6 %). Mice were anesthetized with 70 mg/kg sodium pentobarbital i.p. and the top of the head and nape were topically shaved to reduce optical scatter and signal loss. Consequently, they were injected with DBT (0.3 mg/kg, 0.05 ml/10 g body weight i.v.) *via* tail vein injection. Imaging was performed 5 − 30 min postinjection with the IVIS Lumina II *in vivo* imaging system (PerkinElmer Ltd., Waltham, MA, USA) with a 745 nm excitation and > 800 nm emission filters, auto exposure time, and a binning factor of 2. Fluorescence was expressed as the total or average radiant efficiency ([photons/s/cm^2/steradian]/[μW/cm^2]) of selected regions of interests (ROIs). The FMT 2000 system (PerkinElmer Ltd.) was calibrated using the 750 nm laser channel of the instrument, and a sample solution of 0.5×10^{-6} M following the instructions of the manufacturer. Imaging with the FMT system was performed uniformly 40 min postinjection. Two mice consequently underwent FMT-micro-computer tomography (CT) co-registration. FMT-micro-CT co-registration was successfully used by several studies to locate the fluorescence signal detected by the FMT using reference points of the skeleton and major organs visualized by the micro-CT (Ale et al., 2012; Botz et al., 2015; Khamis et al., 2016; Lin et al., 2012; Stuker et al., 2011). These animals were euthanized with pentobarbital overdose before placing them into the FMT imaging cassette to ensure accurate co-registration and to avoid the need to control for anaesthesia depth. Upon completion of the FMT scan, mice were transferred immediately into the micro-CT (Skyscan 1176, Bruker, Kontich, Belgium) remaining within the imaging cassette, in order to perform a CT-imaging of the head. The FMT and CT datasets were exported as 16-bit DICOM files and were consequently merged together using the AMIDE software. Merging the imaging datasets precisely is possible due to multiple three-dimensional fiducial markers present within the imaging cassette. These show up as coloured spheres in the exported FMT imaging dataset, and are also visible on the CT scans as small holes within the imaging cassette. Thus by aligning the position of fiducial markers on the FMT and CT images in the AMIDE software the two datasets can be accurately combined. Mice not going under multimodal imaging were euthanized with pentobarbital overdose at the end of the FMT scan, at 1 h after DBT injection and dissected for *ex vivo* imaging. Representative organs from the head and neck region, including the brain, salivary glands, muscle, as well as and the sciatic nerve were washed in PBS and imaged with the IVIS Lumina II using the parameters described previously.

2.3. Statistics

Means ± S.E.M. of total or average radiant efficiency values of equal-sized regions of ROIs measured with the IVIS at different time points after DBT injection were calculated. Statistical analysis was performed with GraphPad Prism 6.01. For the evaluation of the time course of *in vivo* dye accumulation, repeated-measures one-way ANOVA followed by Dunnett's multiple comparison test was applied. $p < 0.05$ was considered as statistically significant.

3. Results

3.1. In vivo epifluorescence imaging

Five minutes after DBT injection, a significant increase of fluorescence was measured in the region of interest (ROI) corresponding to the top of the skull. The increased fluorescence could be observed all over the shaved area of the animals' head and neck. The intensity of the fluorescent signal remained significantly elevated compared to the baseline during the measurement period although it declined rapidly throughout the repeated measurements. By the 30-min measurement the total or average radiant efficiency in the skull ROI was less than 50 % of the 5-min value (Fig. 1A, B). Representative images are shown in Fig. 1C.

3.2. FMT-CT co-registration

The FMT detected an area with intense fluorescence in the head and neck region of the animal. For a more accurate anatomical localization, the reconstructed FMT image was merged with the CT scan of the same animal. The reconstruction revealed that the area with the highest signal was on the neck next to the base of the skull, seemingly outside the cranium (Fig. 2.). Lower intensity accumulation was also seen on the dorsal and lateral part of the neck. A short video of the 3D reconstructed image is available as Supplementary material.

3.3. Ex vivo imaging of different organs

Comparing the fluorescence of identically sized ROIs of the brain, sciatic nerve, submandibular salivary gland, as well as muscle and adipose tissue from the neck revealed that the brain and peripheral nerve displayed a very low content of the dye, while the highest signal was detected in the salivary gland (Fig. 3A, B). We also quantified the accumulation of DBT by comparison to organs of untreated mice. The ratio of total radiant efficiency between DBT-treated and intact organs was 4.7 and 2.05 for the brain and sciatic nerve respectively, while in cases of non-nervous tissues these ratios were 12.0, 28.6 and 37.7 for adipose tissue, muscle and salivary gland, respectively (Fig. 3C). Representative images are shown in Fig. 3D.

Since we performed the *ex vivo* imaging before the reconstruction of the FMT-CT co-registration was ready, we did not expect that other structures might be accumulating the dye specifically. Based on the intense signal on the merged FMT-CT image at the base of the skull, we suspected that the dye was also accumulated in the pituitary gland. We decided to sacrifice one additional mouse to confirm the finding with *ex vivo* imaging of the base of the skull as well. As seen on Fig. 3E, we demonstrated that the dye was concentrated in both the anterior and posterior lobes of the pituitary gland.

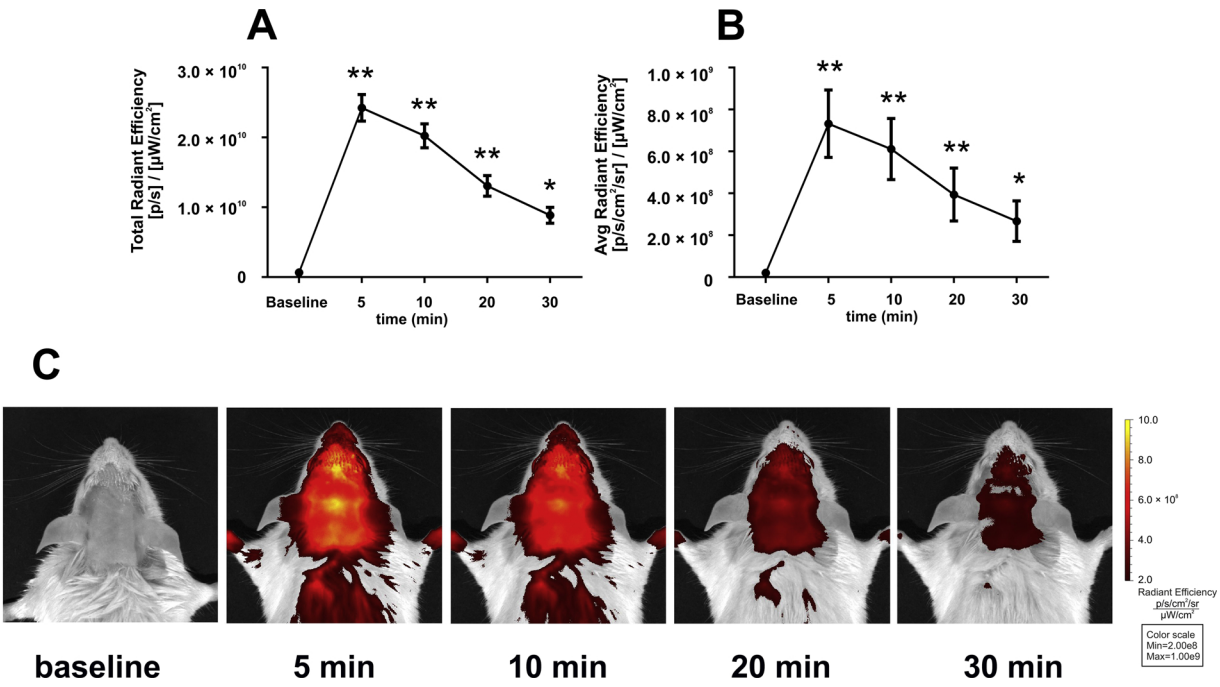

Fig. 1. Epifluorescent imaging of the mouse head before and after injection of 0.3 mg/kg DBT i.v. Fluorescence was measured as total (A) and average radiant efficiency (B) in equal sized regions of interest (ROI) corresponding to the top of the skull. A 745 nm excitation and > 800 nm emission filters, auto exposure time and a binning factor of 2 were used for the imaging. Actual exposure times were 5 − 6 s for baseline, 0.5 s for all 5 and 10 min measurements, 0.5 − 0.75 s for the 20 min and 0.5 − 2 s for the 30 min measurements. Data are means ± S.E.M of 8 animals. Asterisks show statistically significant differences compared to baseline with repeated measures one-way ANOVA followed by Dunnett's test (**p < 0.01, *p < 0.05). Representative images are shown in Panel C. Legends and axis scale numbers have been enhanced with an image editing software for better visibility.

4. Discussion

Non-invasive NIR optical imaging of demyelination could offer a particularly valuable tool for studying various CNS disorders. In the present study we evaluated DBT, as a potential myelin-specific fluorescent dye which was previously reported to be an excellent probe for *in vivo* optical imaging in animal models of multiple sclerosis (Schmitz et al., 2014; Wang et al., 2011). DBT had been demonstrated to have specific binding towards myelin *in vitro*, but according to our results it is completely unsuitable for *in vivo* imaging of de-/remyelination. Our study provided evidence that the compound poorly penetrated the BBB and it did not accumulate in the myelin sheath of peripheral nerves. We also unequivocally demonstrated that the signal localized in the head did not originate from the brain hemispheres, but from the pituitary gland and also from extracranial sources, such as the muscles of the head and neck, as well as the submandibular salivary gland. Thus, even if the dye did bind to myelin *in vivo*, the higher accumulation in adjacent tissues is a significant obstacle to detect the fluorescence from the brain.

For the purpose of our validation study, we used an experimental setup mimicking the one used by previous investigators. In fact, both the time course and the anatomical localization of the fluorescent signal was very similar to those of the previous experiment (Wang et al., 2011). Both our and their results demonstrated that DBT-fluorescence peaks immediately following administration, and decays rapidly thereafter. This is not consistent with tissue-specific dye-accumulation, but more likely follows the time course of the decay of plasma concentration indicating rapid elimination and redistribution from the bloodstream. Moreover, in both previous studies the fluorescence was not restricted to the top of the skull (suggesting accumulation in the brain), but spread evenly to the whole area which was shaved. None of these phenomena corroborated that the dye was accumulating in a

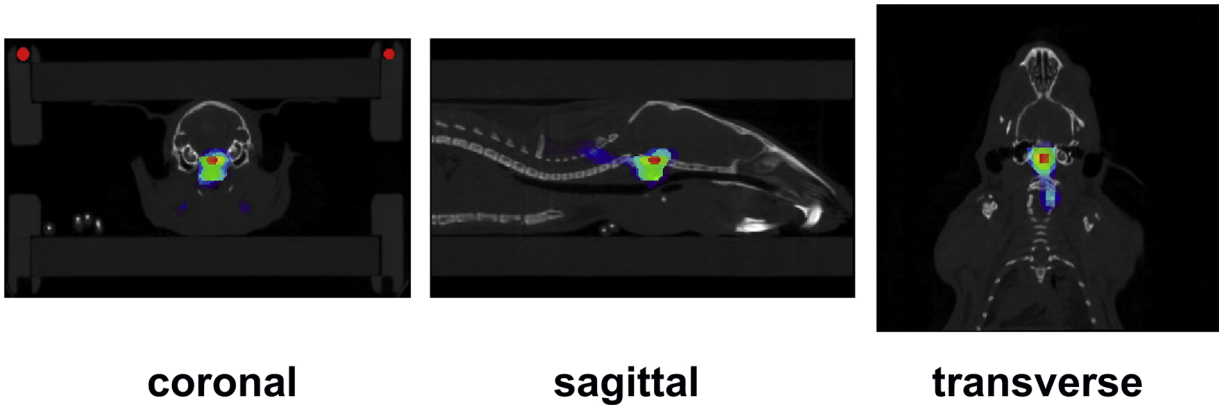

Fig. 2. Images of representative coronal, sagittal and transverse planes of the co-registration with FMT and micro-CT 40 min after DBT injection. See also Supplementary video.

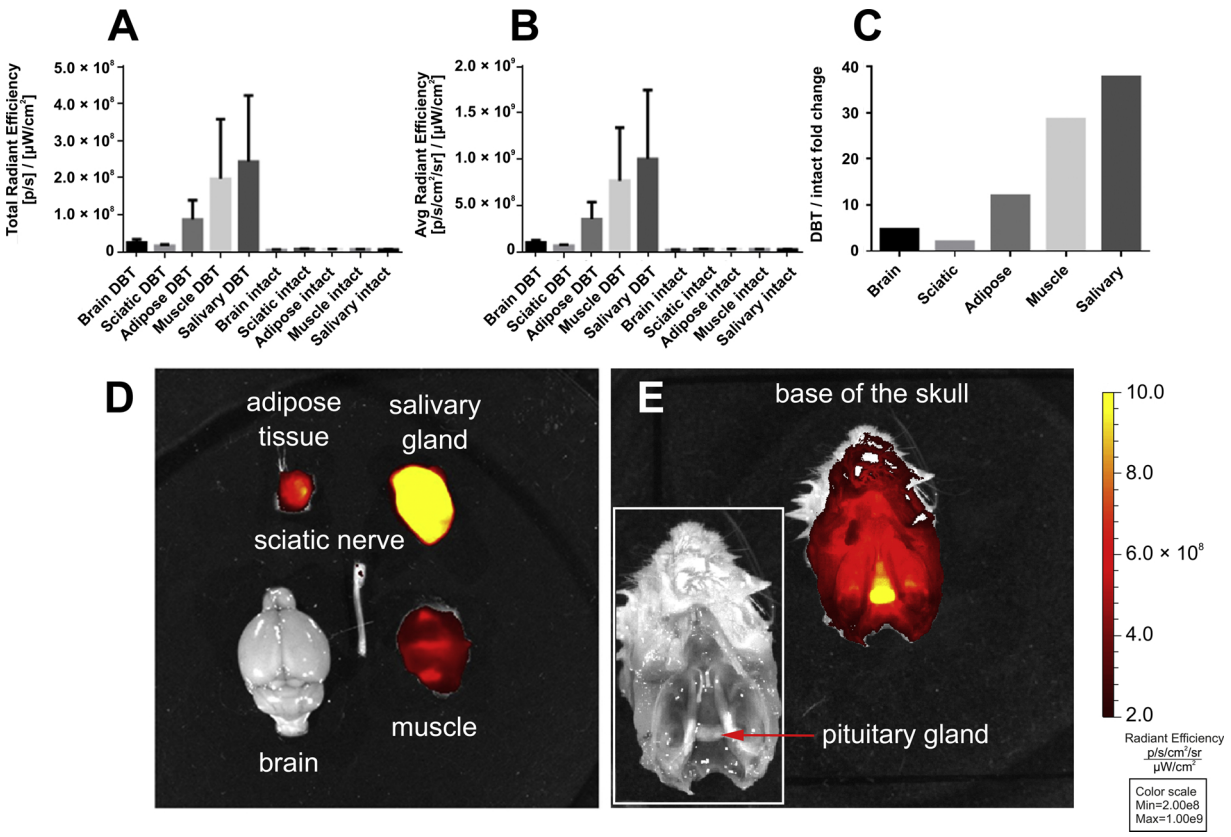

Fig. 3. *Ex vivo* epifluorescent imaging of the brain, sciatic nerve, submandibular salivary gland, as well as muscle and adipose tissue excised from the neck 1 h after DBT injection. Fluorescence was measured as total (A) and average radiant efficiency (B) in equal sized regions of interest (ROI) of each tissue. A 745 nm excitation and > 800 nm emission filters, auto exposure time, and a binning factor of 2 were used for the imaging. Actual exposure times were 7 s for intact and 0.5 s for all DBT-treated tissues. Dye accumulation was also expressed by calculating the fold changes of total radiant efficiency between DBT-treated and intact animals (C). Data are means ± S.E.M of 5 animals. A representative image of the tissues of DBT-treated animals is shown on panel D. Panel E demonstrates the accumulation of the dye in the pituitary gland. Legends and axis scale numbers have been enhanced with an image editing software for better visibility.

tissue-specific manner in the brain, yet the question was not raised if the source of the signal could be other than the nervous tissue.

In the present study, we used two approaches to demonstrate that the observed fluorescence was largely the result of accumulation which overwhelmingly originated from tissues not containing myelin. By the time of these measurements the primary distribution phase of the compound was most probably mainly over, therefore the localization of the dye should reflect tissue affinity. The FMT-CT co-registration clearly demonstrated that most of the signal was localized extracranially and at the base of the skull around the sella turcica. In the previous study, BBB-permeability of DBT was demonstrated using X-ray + epi-fluorescence co-registration (Wang et al., 2011), but these planar imaging modalities do not readily differentiate superficial soft tissue signal sources from the brain. With the *ex vivo* imaging of organs we also showed that there was no specific accumulation either in the brain or in the sciatic nerve. In contrast, the dye was rather accumulating in muscle and surprisingly the pituitary and submandibular salivary gland. The pituitary gland belongs to the brain areas where the BBB is more permeable, therefore, it could have also revealed the myelin-binding property of DBT despite its poor BBB penetration. However, both the anterior and posterior lobes accumulated the dye equally which also questions the *in vivo* myelin-specificity of the dye. Considering the similarly high level of accumulation in the salivary gland, it is very likely that DBT was binding specifically to a protein common in both exocrine and endocrine secretory organs. It must be highlighted that only the FMT and the *ex vivo* imaging could discern the accumulation in the pituitary since it was not detectable separately on the epifluorescent images.

The accumulation in muscle and adipose tissue could offer an explanation for the apparent “demyelination” detected by the method in the multiple sclerosis models, since these models are characterized by loss of body weight (Ács and Kálmán, 2012; Bittner et al., 2014; Praet et al., 2014) and probably muscle mass, as well.

The poor BBB penetration could also be explained by analysing the pharmacokinetics of the compound more closely. The authors of the first imaging study (Wang et al., 2011) only took into consideration the lipophilicity of the compound and concluded that a compound having a logP of 3.04 crosses the BBB. Indeed, this is in accordance with the physicochemical criteria of BBB-penetrating compounds. However, additional factors should also be considered. Paradoxically, high lipophilicity could also result in a high extent of peripheral tissue uptake, which could limit the BBB penetration of the compound. Moreover, other molecular characteristics, such as molecular weight, the number of hydrogen bonds and pharmacokinetic parameters such as plasma protein binding and active transport mechanisms also influence the uptake of drugs into the brain (Banks, 2009; Pardridge, 2012). In fact, there are experimental data showing that DBT demonstrates significant blue-shift of absorbance upon binding to albumin (745–566 nm), which indicates specific dye-albumin interactions (Andrews-Wilberforce and Patonay, 1990). According to a free online tool which predicts the pharmacokinetic properties (https://preadmet.bmdrc.kr) DBT has a plasma protein binding of 97.24 % with a predicted brain:blood ratio of 0.12. Based on our imaging data, the actual BBB penetration seems to be even lower than that, probably due to the high level of peripheral tissue accumulation.

5. Conclusion

In summary, according to our results DBT is unsuitable for *in vivo* imaging of myelination, due to its poor BBB penetration, but also because it does not show selective binding towards myelin *in vivo* compared to other tissues. We conclude that its utility for *in vivo* myelin imaging was disproved; however, the newly discovered specific accumulation in glands could potentially be exploited for the study of endocrine diseases.

Author contribution statement

Bálint Botz: Conceptualization, Methodology, Formal analysis, Investigation, Writing - Original Draft, Writing - Review & Editing, Visualization.

István Zoárd Bátai: Investigation, Writing - Original Draft, Writing - Review & Editing, Visualization.

Tamás Kiss: Methodology, Formal analysis, Investigation, Writing - Original Draft, Writing - Review & Editing, Visualization.

Erika Pintér: Conceptualization, Writing - Original Draft, Writing - Review & Editing, Supervision, Funding acquisition.

Zsuzsanna Helyes: Conceptualization, Writing - Original Draft, Writing - Review & Editing, Supervision, Funding acquisition.

Kata Bölcskei: Conceptualization, Methodology, Formal analysis, Investigation, Writing - Original Draft, Writing - Review & Editing, Visualization, Supervision.

Declaration of Competing Interest

None.

Acknowledgements

This work was supported by grants EFOP-3.6.1-16-2016-00004, "Stay Alive" GINOP-2.3.2.-15-2016-00048, Hungarian Brain Research Program2. 2017-1.2.1-NKP-2017-00002. and University of Pécs Medical School grant KA-2015-20. Bálint Botz was supported by the János Bolyai Research Scholarship of The Hungarian Academy of Sciences and the ÚNKP-19-4-P-PTE-458New National Excellence Program of the Ministry for Innovation and Technology.

Appendix A. Supplementary data

Supplementary material related to this article can be found, in the online version, at doi:https://doi.org/10.1016/j.brainresbull.2019.12.009.

References

Ács, P., Kálmán, B., 2012. Pathogenesis of multiple sclerosis: what can we learn from the cuprizone model. In: Perl, A. (Ed.), Autoimmunity. Humana Press, Totowa, NJ, pp. 403–431.

Ale, A., Ermolayev, V., Herzog, E., Cohrs, C., de Angelis, M.H., Ntziachristos, V., 2012. FMT-XCT: in vivo animal studies with hybrid fluorescence molecular tomography–X-ray computed tomography. Nat. Methods 9, 615–620. https://doi.org/10.1038/nmeth.2014.

Andrews-Wilberforce, D., Patonay, G., 1990. Investigation of near-infrared laser dye albumin complexes. Spectrochim. Acta Part A: Mol. Spectrosc. 46, 1153–1162. https://doi.org/10.1016/0584-8539(90)80191-Z.

Banks, W.A., 2009. Characteristics of compounds that cross the blood-brain barrier. BMC Neurol. 9, S3. https://doi.org/10.1186/1471-2377-9-S1-S3.

Bittner, S., Afzali, A.M., Wiendl, H., Meuth, S.G., 2014. Myelin oligodendrocyte glycoprotein (MOG35-55) induced experimental autoimmune encephalomyelitis (EAE) in C57BL/6 mice. J. Vis. Exp. https://doi.org/10.3791/51275.

Botz, B., Bölcskei, K., Kemény, Á., Sándor, Z., Tékus, V., Sétáló, G., Csepregi, J., Mócsai, A., Pintér, E., Kollár, L., et al., 2015. Hydrophobic cyanine dye-doped micelles for optical in vivo imaging of plasma leakage and vascular disruption. J. Biomed. Opt. 20 016022–016022.

Hillman, E.M.C., 2007. Optical brain imaging in vivo: techniques and applications from animal to man. J. Biomed. Opt. 12, 051402. https://doi.org/10.1117/1.2789693.

Khamis, R.Y., Woollard, K.J., Hyde, G.D., Boyle, J.J., Bicknell, C., Chang, S.-H., Malik, T.H., Hara, T., Mauskapf, A., Granger, D.W., Johnson, J.L., Ntziachristos, V., Matthews, P.M., Jaffer, F.A., Haskard, D.O., 2016. Near infrared fluorescence (NIRF) molecular imaging of oxidized LDL with an autoantibody in experimental atherosclerosis. Sci. Rep. 6, 21785. https://doi.org/10.1038/srep21785.

Lin, S.-A., Patel, M., Suresch, D., Connolly, B., Bao, B., Groves, K., Rajopadhye, M., Peterson, J., Klimas, M., Sur, C., Bednar, B., 2012. Quantitative longitudinal imaging of vascular inflammation and treatment by ezetimibe in apoE mice by FMT using new optical imaging biomarkers of cathepsin activity and αvβ3 integrin. Int. J. Mol. Imaging 2012, 189254. https://doi.org/10.1155/2012/189254.

Pardridge, W.M., 2012. Drug transport across the blood–brain barrier. J. Cereb. Blood Flow Metab. 32, 1959–1972. https://doi.org/10.1038/jcbfm.2012.126.

Praet, J., Guglielmetti, C., Berneman, Z., Van der Linden, A., Ponsaerts, P., 2014. Cellular and molecular neuropathology of the cuprizone mouse model: clinical relevance for multiple sclerosis. Neurosci. Biobehav. Rev. 47, 485–505. https://doi.org/10.1016/j.neubiorev.2014.10.004.

Schmitz, K., de Bruin, N., Bishay, P., Männich, J., Häussler, A., Altmann, C., Ferreirós, N., Lötsch, J., Ultsch, A., Parnham, M.J., Geisslinger, G., Tegeder, I., 2014. R-flurbiprofen attenuates experimental autoimmune encephalomyelitis in mice. EMBO Mol. Med. 6, 1398–1422. https://doi.org/10.15252/emmm.201404168.

Stuker, F., Ripoll, J., Rudin, M., 2011. Fluorescence molecular tomography: principles and potential for pharmaceutical research. Pharmaceutics 3, 229–274. https://doi.org/10.3390/pharmaceutics3020229.

Wang, C., Wu, C., Popescu, D.C., Zhu, J., Macklin, W.B., Miller, R.H., Wang, Y., 2011. Longitudinal near-infrared imaging of myelination. J. Neurosci. 31, 2382–2390. https://doi.org/10.1523/JNEUROSCI.2698-10.2011.

Willmann, J.K., Bruggen, N., Dinkelborg, L.M., Gambhir, S.S., 2008. Molecular imaging in drug development. Nat. Rev. Drug Discov. 7, 591–607. https://doi.org/10.1038/nrd2290.